

METAMORPHIC CONDITION

PART A- GEOTHERMOMETRY AND GEOBAROMETRY

7.A.1 Introduction

Geothermometry and geobarometry models play a significant role in determining pressure-temperature (P-T) conditions in the field of metamorphic rocks. However, estimating these conditions can be quite challenging when dealing with rocks that have undergone polymetamorphic events. This complexity arises from the fact that the mineral compositions within these rocks may change as they cool involving cation exchanges that impact their final composition. It is well-established that interpreting mineral compositions in metamorphic rocks is challenging, particularly when attempting to capture the equilibrium distributions of all elements of interest under peak metamorphic conditions. This variability in composition, which is difficult to quantify, has a more pronounced impact on the accuracy and precision of thermobarometry models. During the process of metamorphism, the minerals and textures within rocks change over time in response to pressure, temperature, and time. The highest temperature point, known as the thermal peak condition of metamorphism, is especially important because the reaction kinetics is highly sensitive to temperature. Using geothermometry and geobarometry models to identify these key points can be helpful, but the accuracy of the results depends on the interpretation of mineral textures and mixing models used in geothermometers.

7.A.2 Thermodynamic Basis

The concept behind 'geothermobarometry' is easy to understand. This term

Metamorphic Condition

refers to using the pressure and temperature impact on the equilibrium constant to determine the metamorphic temperatures and pressures of equilibration. The basic standard for this is a thermodynamic expression that states:

$$\Delta G(P, T, X) = 0 = \Delta H(298,1) + \int_{298}^T \Delta C_p dT + \int_1^P \Delta V dP - T[\Delta S(298,1) + \int_{298}^T (\Delta C_p / T) dT] + RT \ln K \dots (1)$$

Where, ΔS : change in entropy, ΔH : change in enthalpy, ΔV : volume change, C_p : heat capacity, dP : change in pressure, R : gas constant=1.987 cal, T : absolute temperature in Kelvin, P : pressure in bars.

To determine the equilibrium constant of a sample, the mineral compositions of coexisting minerals are analyzed using microprobes. The standard state equation (1) and its thermodynamic parameters are discussed in depth in fundamental thermodynamics textbooks, providing a comprehensive understanding of their inter-relationship.

7.A.3 Presumption

When using geothermobarometry, it is assumed that the mineral phases are in equilibrium. This means that a heterogeneous system in a metamorphic rock is in a state of equilibrium. Although it is possible to show that an assemblage is not in equilibrium, determining whether phases in a rock developed in equilibrium is more challenging. All thermodynamic relationships and derivations are based on the concept of equilibrium, but thermodynamics itself does not provide criteria for determining equilibrium. Instead, it describes the characteristics of equilibrium. Therefore, to apply thermodynamics, this concept must be accepted.

Geothermobarometers The determination of the conditions under which rocks are formed, including temperature and pressure, is known as geothermometry and geobarometry, collectively referred to as geothermobarometry. Geothermobarometry relies on the mineral composition of rocks and chemical reactions that are highly sensitive to temperature (large ΔH , ΔS) but less sensitive to pressure (large ΔV). In contrast, geobarometers involve reactions that are significantly sensitive to pressure (large ΔV) but less sensitive to temperature (small ΔH and ΔS). Geothermobarometers utilize thermodynamic equations with small ΔV and large ΔS , while geobarometers use expressions with high low ΔS and ΔV . As a result, geothermometers align more closely with the pressure axis, while ideal geobarometers align with the temperature axis in the P–T diavariant field. Vapor-absent, solid-solid reactions are ideally suited for geobarometry. Geothermobarometers typically rely on two types of calibrations. Empirical calibrations are based on equilibrium constants derived from natural data, while experimental calibrations involve measurements of equilibrium constants under controlled laboratory conditions with varying temperatures and pressure. Experimental calibrations are considered more accurate because they provide better control over the equilibrium constant and dependence on pressure and temperature. Empirical calibrations, on the other hand, incorporate non-ideality in solid solution phases but are not as precise as experimental calibrations because they rely on calibration from different sources for temperature and pressure assessment. There are two types of thermometers: exchange geothermometers and solvus thermometers. Exchange geothermometers focus on ion exchange reactions (e.g., Fe-Mg; Fe-Ti) between coexisting silicates, characterized by large ΔS and small ΔV , resulting in steep isopleths of equilibrium constants. The distribution coefficient

Metamorphic Condition

(K_D) is used to describe the partitioning of elements between minerals. For instance K_D for the FeMg-1 exchange reaction between garnet and biotite is defined as $K_D = [\text{Fe}/\text{Mg}]_{\text{Grt.}} / [\text{Mg}/\text{Fe}]_{\text{Bt.}}$. Solvus thermometers rely on the compositional variability of structurally linked phases in the T-X space miscibility gap (solvus). Since miscibility gaps are temperature-dependent, they are mainly used as thermometers. Solvus thermometry is applied to mineral pairs like plagioclase-alkali feldspar and orthopyroxene-clinopyroxene.

In geobarometry, potential geobarometers involve solid-solid, vapour-absent reactions with significant volume changes and a slight positive slope in P–T space. These equilibria provide pressure estimates using temperatures obtained from the exchange or other thermometers. Garnet-based geobarometers are frequently used due to garnet's refractory nature. However, using different activity models for common anhydrous phases like orthopyroxene, plagioclase, and garnet can lead to discrepancies in calculated P– T conditions. Spear (1989) and Essene (1989) provide comprehensive syntheses of these geobarometric methods.

7.A.4 Errors/Problem in Geothermobarometry

Any scientific field that relies on quantitative measurements, such as geothermobarometry, necessitates a careful examination of error propagation. Nevertheless, thermobarometry is not exempt from its challenges and conducting calculations without considering some form of uncertainty estimation renders the results meaningless. Consequently, petrologists have found the outcomes of geothermobarometry to be only partly satisfactory. To ascertain metamorphic conditions with utmost precision based on highly accurate data, petrologists are

currently developing new calibration methods to attain ideal geothermobarometry models. Hodges and McKenna (1987) and Spear (1989) have extensively explored significant factors contributing to error sources in thermobarometry. Below, we summarize various error sources and problems encountered in thermobarometry.

7.A.4.1 Evaluation of Chemical Equilibrium

A fundamental prerequisite for thermobarometry is assuming that chemical equilibrium exists among the different phases. Hence, it is advantageous to search for sub-groups within various domains of the same rock that display either local equilibrium or mosaic equilibrium. This approach allows us to confirm or deny whether equilibrium is present. Consequently, the inability to pass certain tests designed to detect disequilibrium in a rock indirectly verifies the equilibration condition. One straightforward method involves examining the topological projections of the selected assemblage's tie-lines, and equilibrium is indicated when these tie-lines do not intersect. Another test involves assessing the distribution of elements between a pair of coexisting minerals. Whether the distribution pattern follows a systematic or random trend provides insight into whether equilibrium or disequilibrium prevails. The patterns of mineral zoning (composition profiles) serve as a means to determine which component of the zoned mineral is in equilibrium condition with the surrounding matrix phase of the rock.

7.A.4.2 Re-equilibration during Retrogression

Thermobarometric calculations typically provide information on the peak metamorphic conditions only in specific cases. Most of the time, they indicate lower temperatures due to re-equilibration during retrogression. Studies on cationic

exchange equilibria suggest that the rim compositions of garnet in contact with biotite show signs of significant Fe-Mg resetting preventing accurate recording of peak temperatures. Even utilizing Fe-Mg exchange thermometry on refractory phases like the core composition of orthopyroxene and garnet grain may not capture the peak conditions due to resetting (Pattison & Begin, 1994a, b). Additionally, two-feldspar thermometers often yield lower temperatures because of the exsolution property. Bohlen & Essene (1977) employed a reintegration method for exsolved lamellae to achieve geologically appropriate temperatures.

7. A.5.3 Quality of Thermobarometric Formulations

There are two types of computations: thermodynamic and experimental. Despite significant advancements in our understanding of mineral thermodynamics and calorimetric information, our knowledge remains incomplete. Frequently, adjustments for volume changes in solid-solid equilibria are neglected. Inadequate mixing models, substantial thermodynamic differences between the natural mineral and its less suitable counterpart or synthetic phase, and experimental data lacking tightly constrained and corroborating results can all undermine the quality of the calibration.

7. A.5.4 Extrapolations

At extremely high P - T settings the number of reaction equilibria has been investigated experimentally. To apply these equilibria at much lower P - T conditions an extended projection reaction slope in an area outside the critical limits is required, which is a risky inference. Calculations of propagating uncertainty are unexpectedly large in such instances.

7. A.5.5 Sensitivity and Constraints of Thermobarometers

Many thermobarometric methods have limitations in terms of the range of pressure and temperature they can accurately assess. For instance, the commonly used garnet-biotite exchange equilibria serve as a geothermometer and have been calibrated in about 18 different ways. Some of these calibrations explicitly specify that they are applicable only within certain compositional limits. In their research work, Ferry & Spear (1978) restricted their ideal mixing model to rocks containing low Ca and Mn garnets. In contrast, Hodges & Spear (1982) and Perchuk & Lavrent'eva (1983) incorporated adjustments for the Grossular component in garnet, which is known to exhibit non-ideal mixing with pyrope. Consequently, their calibrations yield higher temperature estimates as compared to those of Ferry & Spear (1978).

7. A.5.6 Analytical errors in Microprobe data

The electron microprobe method has a notable limitation in that it can only provide information about the total iron content. To determine the proportions of Fe^{2+} and Fe^{3+} , researchers rely on ideal structural formulas and various adjustment processes. Regrettably, these recalculations based on stoichiometry are quite sensitive to even minor errors in the measurement of SiO_2 and Al_2O_3 , especially when the Fe^{3+} content is low. Model temperatures are often calculated using Fe-Mg distribution equilibria based on the total iron content. However, when considering only Fe^{2+} , these temperature estimates can deviate by as much as 100°C .

7. A.5.7 Effect of other components in solid solutions

In general, thermobarometers rely on mineral chemistry but many naturally occurring minerals exhibit a noticeable tendency toward intricate solid solutions. To

Metamorphic Condition

determine the ideal end-member within these complex solid solutions, various methods can be employed, and the choice of method depends on the structural formulae as well as the quality of analyses. It's crucial to have accurate knowledge of both Fe²⁺ and Fe³⁺ contents when applying these recasting procedures.

7. A.5.8 Effect of cation order/disorder

Cation disorder plays a significant role in thermobarometry. Experimental data regarding sapphirine stability indicates the presence of a metastable disordered phase, whereas this phase exhibits orderliness in naturally cooled samples that cool gradually. To effectively use sapphirine reactions for more accurate quantitative thermobarometry further research in crystal chemistry concerning this material is essential.

7. A.5.9 Error Analyses

It combines the precision and accuracy of pressure and temperature measurements and requires a comprehensive examination before establishing a meaningful interpretation in thermobarometry. For instance, in the case of most geobarometers, the total uncertainty in pressure may arise from a series of independent error sources. The total pressure uncertainty (σ_P -total) comprises three components: statistical uncertainty (σ_P -statistical), uncertainty due to sample heterogeneity (σ_P sample heterogeneity) and uncertainty associated with activity models (σ_P activity models). Numerous researchers have provided detailed assessments of how uncertainty propagates in thermobarometry (Hodges and McKenna, 1987). Precision refers to the reproducibility of measurements and accounts for errors that are randomly distributed. It primarily relates to the analytical

uncertainty encountered during electron microprobe analyses. On the other hand, the accuracy of the Pressure–Temperature measures how closely the estimate aligns with the actual Pressure–Temperature conditions. However, estimating the accuracy of the Pressure–temperature estimate can be challenging because the error sources contributing to it are not well constrained.

7. A.5.10 Blocking temperature effect

Ongoing reactions have the potential to reconfigure thermobarometric measurements as rocks undergo cooling after reaching their peak metamorphic conditions. As the temperature progressively decreases, these reactions eventually come to a halt. The temperature at which a thermometer records its last data point after being reset during cooling is referred to as the blocking temperature. When applying thermometry to high-grade metamorphic rocks, it is important to consider that most cation exchange thermometers have blocking temperatures lower than those found in the granulite facies, making them susceptible to resetting as the rocks cool down.

**PART B - APPLICATION OF GEOTHERMOBAROMETERS AND
AVERAGE P-T**

Understanding the thermal state of the lithospheric mantle in the past or present requires an accurate estimation of the P - T conditions. Naturally, precise and exact thermometers and barometers are necessary to get dependable P - T calculations (Tam et al., 2012). The various geothermobarometry models provide estimated pressure and temperature conditions, which are visualized in diagrams and described as follows and illustrated in Figures 7.1-7.10:

7. B.1 Pelitic granulite

The various conventional geothermobarometry pairs such as garnet-biotite and garnet-cordierite geothermometers and garnet-biotite-plagioclase-quartz and garnet-cordierite-sillimanite-quartz geobarometers have been used for evaluating the temperature and pressure conditions for pelitic granulites. Table 7.1 represents the temperature and pressure estimates of pelitic granulites with various proposed models. For the pelitic granulite, the estimated temperature by Garnet-Biotite thermometry provides prograde temperatures of 690 ± 62 °C at a fixed pressure of 6 kbar (because this value of pressure was observed within the mafic granulite adjacent to the study area by Pandey et al.2022). Whereas, a pressure of 6.2 kbar at 600°C using the garnet-biotite-plagioclase-quartz geobarometer (GBPQ). Similarly, the garnet-cordierite geothermometer provides the retrograde temperature of 575 ± 28 °C at a fixed pressure of 5 kbar, whereas the garnet-cordierite-sillimanite-quartz geobarometer was used to estimate the pressure of 5.55 ± 0.73 kbar at 600°C. The average P-T conditions of Pelitic granulites are estimated using an internally consistent thermodynamic dataset of

(Holland and Powell(2011) with the help of THERMOCALC software 3.21 (Powell and Holland, 1988). The average PTcondition was estimated with coexisting phases involving garnet, biotite, plagioclase, cordierite and sillimanite is 679 ± 63 °C/ 5.3 ± 0.9 kbar for an (H₂O) = 1.

7. B.2 Garnet bearing gneiss

P-T conditions of the garnet-bearing gneisses were calculated using conventional garnet– biotite exchange geothermometers and garnet-biotite-plagioclase-quartz geobarometers (Table 5). The peak temperature of the Garnet bearing gneiss (M-1) was calculated using conventional garnet–biotite exchange geothermometers are 566 ± 33 °C at a fixed pressure of 6 kbar and pressure conditions were calculated using conventional garnet- biotite-plagioclase-quartz geobarometers of (Hoisch et al., 1990) which provides a pressure estimate of 5.11 kbar at 600°C.

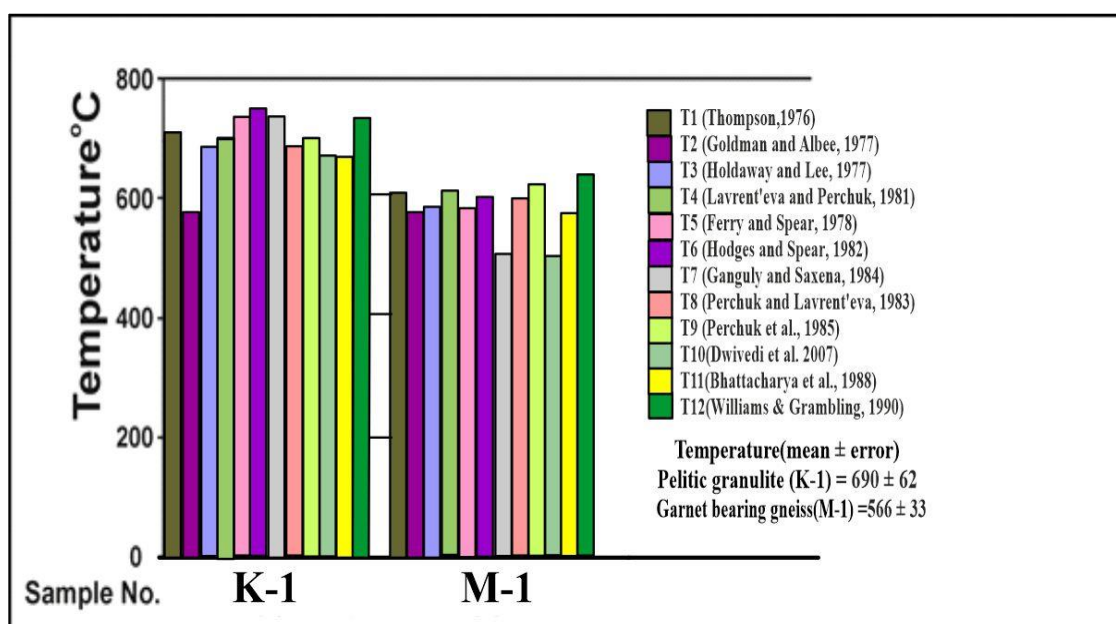


Figure 7.1 Coexisting Garnet-biotite pairs and derivative temperatures for different rocks.

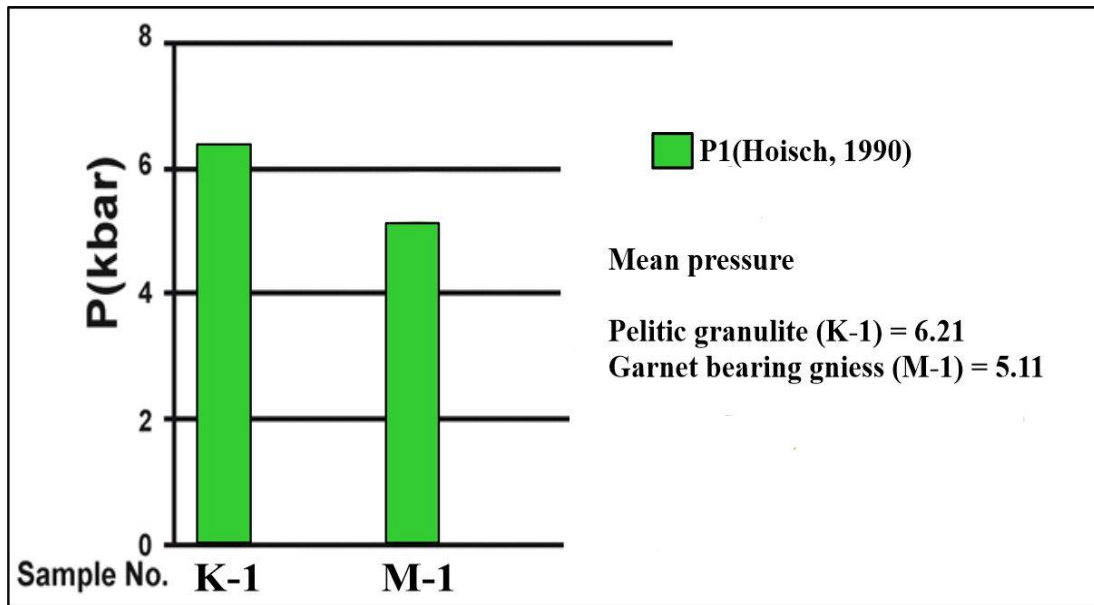


Figure 7.2 Coexisting Garnet-biotite pairs and derivative pressures for different rocks.

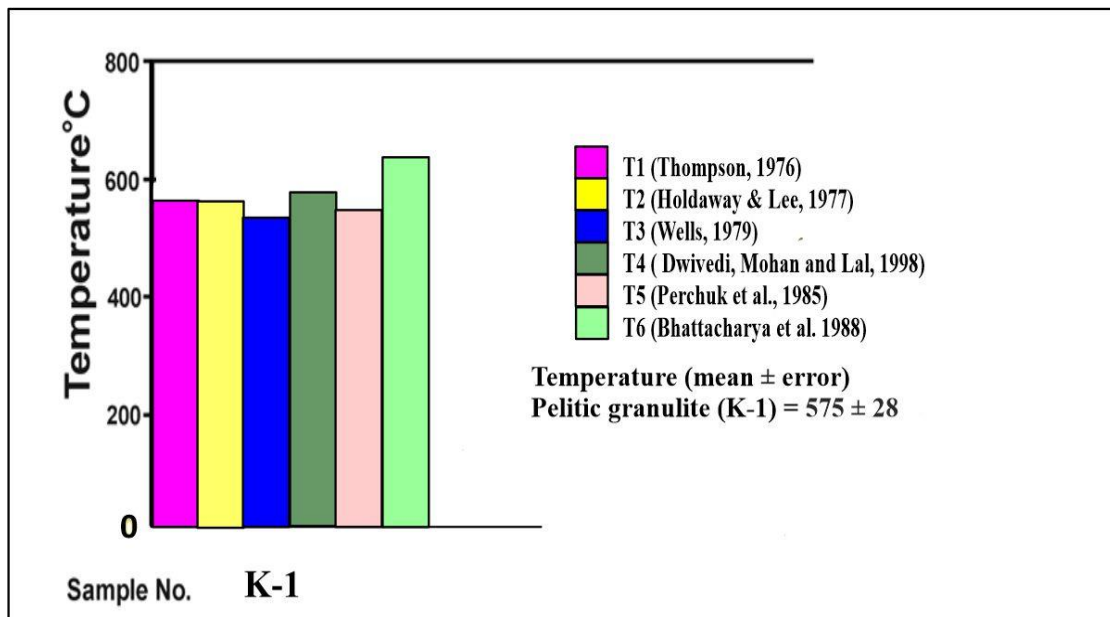


Figure 7.3 Coexisting Garnet-Cordierite pairs and derivative temperatures for pelitic granulites.

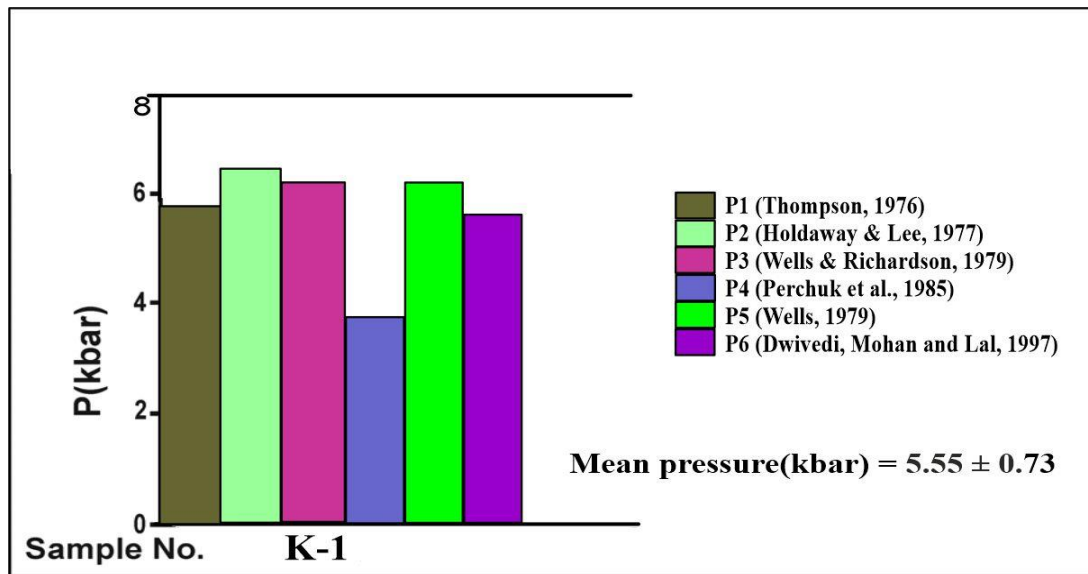


Figure 7.4 Coexisting Garnet-Cordierite pairs and derivative pressures for pelitic granulites.

7.B.3 Calc-silicate granulites

The temperature and pressure conditions of their formation have been estimated with the help of conventional garnet–clinopyroxene exchange geothermometers and garnet–clinopyroxene–plagioclase–quartz geobarometers. The temperature estimates through garnet-clinopyroxene exchange thermometer of the calc-silicate granulites of the study area is 675 ± 89 °C at a fixed pressure of 7 kbar and pressure is 5.55 ± 0.74 kbar at 600 °C is given in Table 7.3. The average P-T conditions of calc-silicate granulites are estimated using an internally consistent thermodynamic dataset of (Holland and Powell (2011) with the help of THERMOCALC software 3.21 (Powell and Holland, 1988). The average PT condition was estimated with coexisting phases involving garnet, clinopyroxene, plagioclase, clinozoisite and quartz is 624 ± 97 °C/ 5.6 ± 0.8 kbar for an $(H_2O) = 1$.

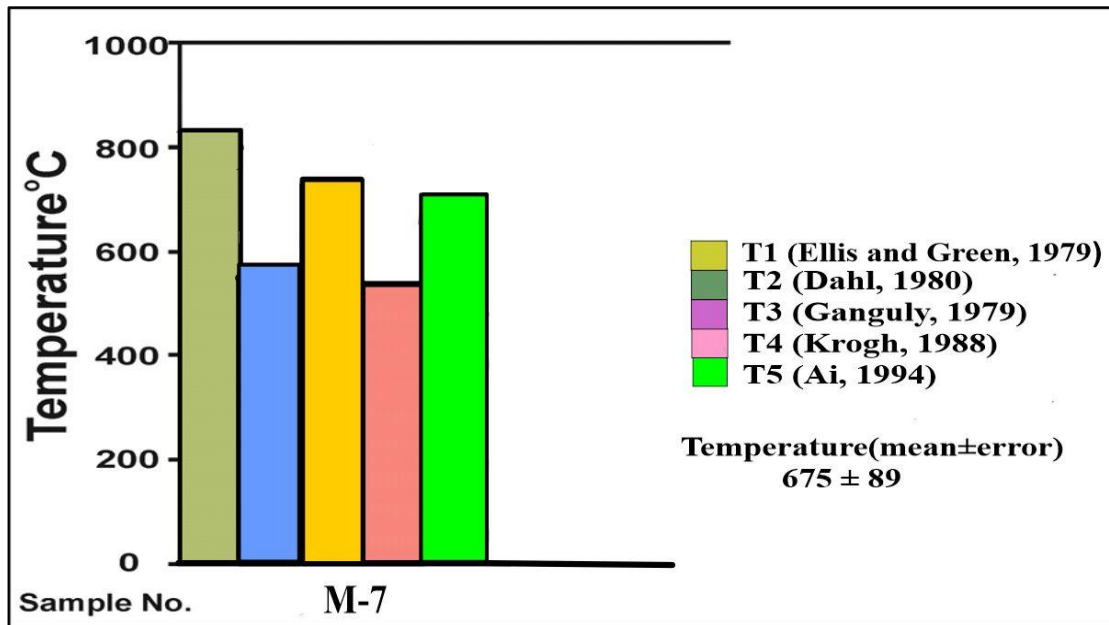


Figure 7.5 Coexisting Garnet-Clinopyroxene pairs and derivative temperatures for calc-silicate granulites.

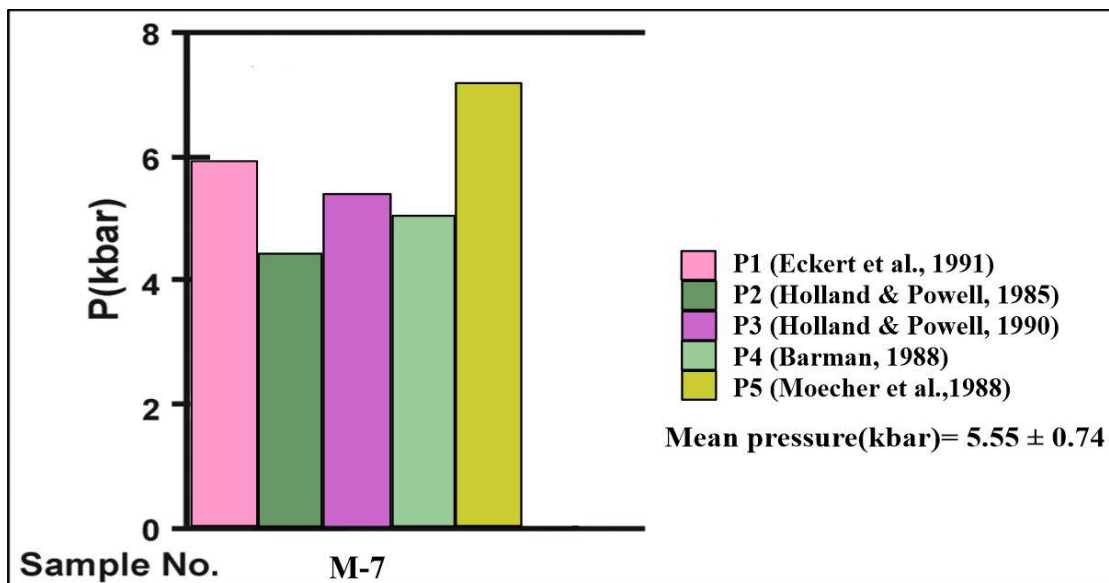


Figure 7.6 Coexisting Garnet-Clinopyroxene pairs and derivative pressures for calc-silicate granulites.

7.B.4 Mafic granulites

P–T conditions of the mafic granulites were determined using orthopyroxene–clinopyroxene conventional exchange geothermobarometers. The peak temperature estimates of coexisting orthopyroxene–clinopyroxene of the study area was $887^{\circ} \pm 62^{\circ}\text{C}$ at a fixed pressure of 6 kbar. The pressure condition of the prograde

metamorphic stage was obtained using the two-pyroxene barometer of Mercier et al. (1984), which provided an estimate of 6.15 ± 0.3 kbar. For the post-peak metamorphic stage, texturally equilibrated mineral assemblages Hbl2, Pl and Qz were selected to determine their P–T conditions. The pressure condition of the post-peak metamorphic stage was obtained using the aluminium-in-amphibole barometer of Schmidt (1992), which provided an estimate of 2.28 ± 0.15 kbar. The temperature estimates of the Hbl–Pl–Qz thermometer of Holland and Blundy (1994), at pressure obtained using the aluminium-in-amphibole barometer of Schmidt (1992) suggest an estimate of $593 \pm 50^\circ\text{C}$ (Table 7.2).

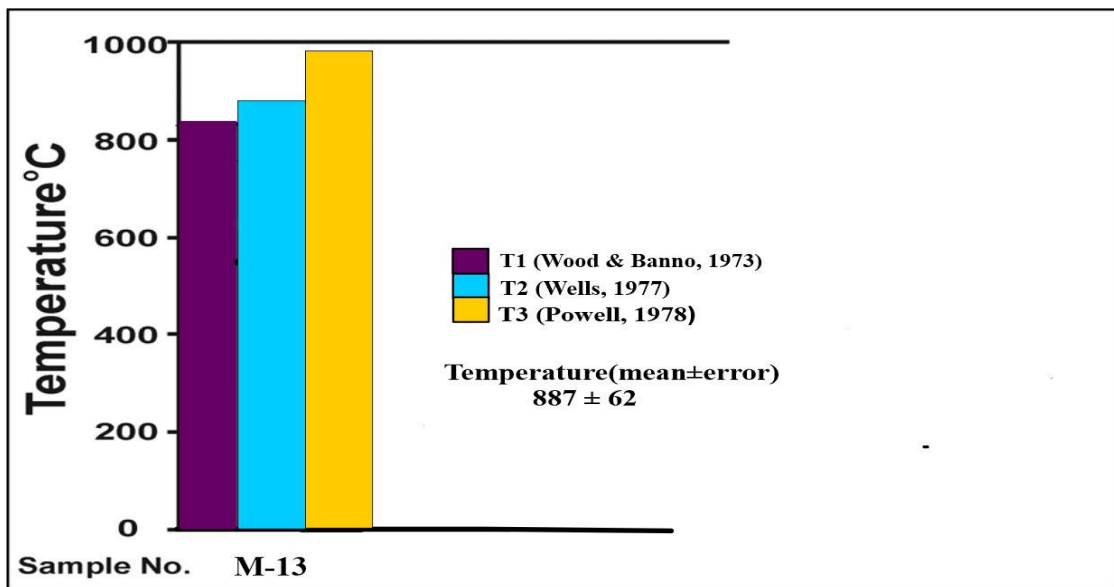


Figure 7.7 Coexisting Orthopyroxene-Clinopyroxene pairs and derivative temperatures for mafic granulites.

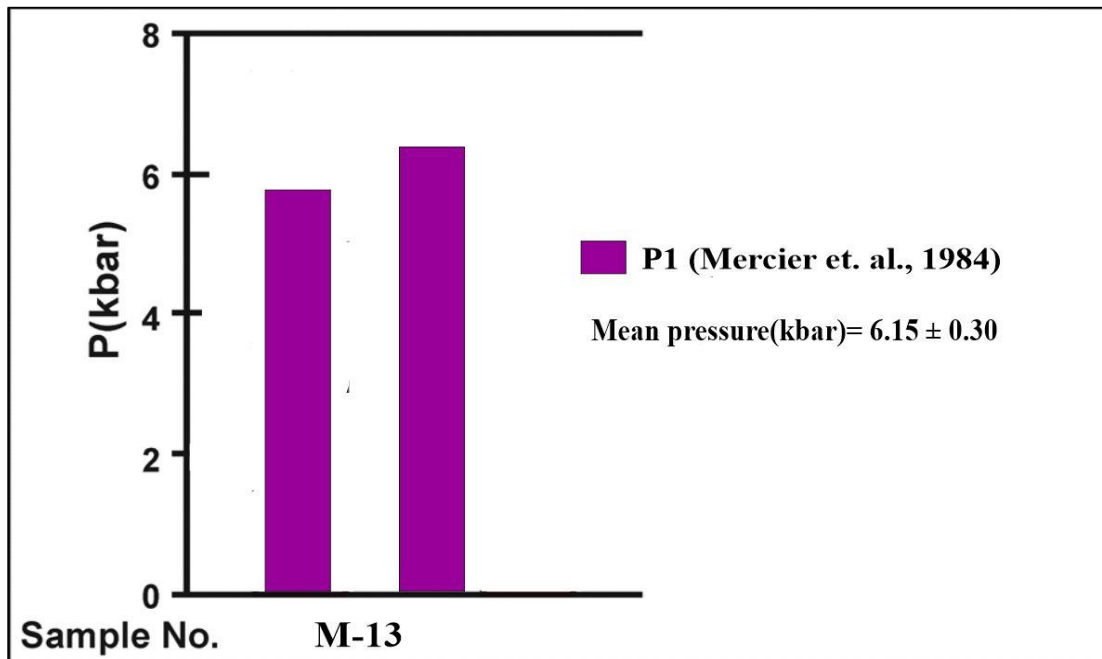


Figure 7.8 Coexisting Orthopyroxene-Clinopyroxenes pairs and derivative pressures for mafic granulites.

7.B.5 Amphibolites

We aimed to determine the pressure-temperature (P-T) conditions at different stages of metamorphism in amphibolites, a critical aspect for comprehending the metamorphic evolution of these rocks. Various geothermobarometry models were employed to estimate the pressure and temperature conditions for amphibolites and these results are summarized in Table 7.4. In garnetiferous amphibolites, for the peak metamorphic stage, the Grt-Cpx geothermometer yielded temperature estimates of 643 ± 51 °C at a pressure of 5.0 kbar. The pressure condition of the peak metamorphic stage was obtained using the garnet-clinopyroxene-plagioclase-quartz geobarometers, which provided an estimate of 5.62 ± 0.62 kbar. For the post-peak metamorphic stage, texturally equilibrated mineral assemblages Hbl, Pl and Qz were selected to determine their P-T conditions. The pressure condition of the post-peak metamorphic stage was obtained using the aluminium-in-amphibole barometer of

Schmidt (1992), which provided an estimate of 4.30 ± 0.28 kbar. The temperature estimates of the Hbl–Pl–Qz thermometer of Holland and Blundy (1994), at pressure obtained using the aluminium-in-amphibole barometer of Schmidt (1992) suggest an estimate of $612 \pm 28^\circ\text{C}$ (Table 7.4). In garnet absent amphibolites, the retrograde metamorphic condition texturally equilibrated mineral assemblages Hbl, Pl and Qz were selected to determine their P–T conditions. The pressure condition of the retrograde metamorphic condition was obtained using the aluminium-in-amphibole barometer of Schmidt (1992), which provided an estimate of 5.26 ± 0.21 kbar. The temperature estimates of the Hbl–Pl–Qz thermometer of Holland and Blundy (1994), at pressure obtained using the aluminium-in-amphibole barometer of Schmidt (1992) suggest an estimate of $620 \pm 42^\circ\text{C}$ (Table 7.4). The average P-T conditions of amphibolites are estimated using an internally consistent thermodynamic dataset of (Holland and Powell (2011) with the help of THERMOCALC software 3.21 (Powell and Holland, 1988). The average PT condition of garnetiferous amphibolite was estimated with coexisting phases involving garnet, biotite, clinopyroxene, amphibole and plagioclase is $706 \pm 63^\circ\text{C}/5.5 \pm 0.9$ kbar for an $(\text{H}_2\text{O}) = 1$ (Table 7.4). The average PT condition of garnet absent amphibolite was estimated with coexisting phases involving clinopyroxene, biotite, amphibole and plagioclase as $616 \pm 81^\circ\text{C}/5.2 \pm 0.7$ kbar for an $(\text{H}_2\text{O}) = 1$ (Table 7.4).

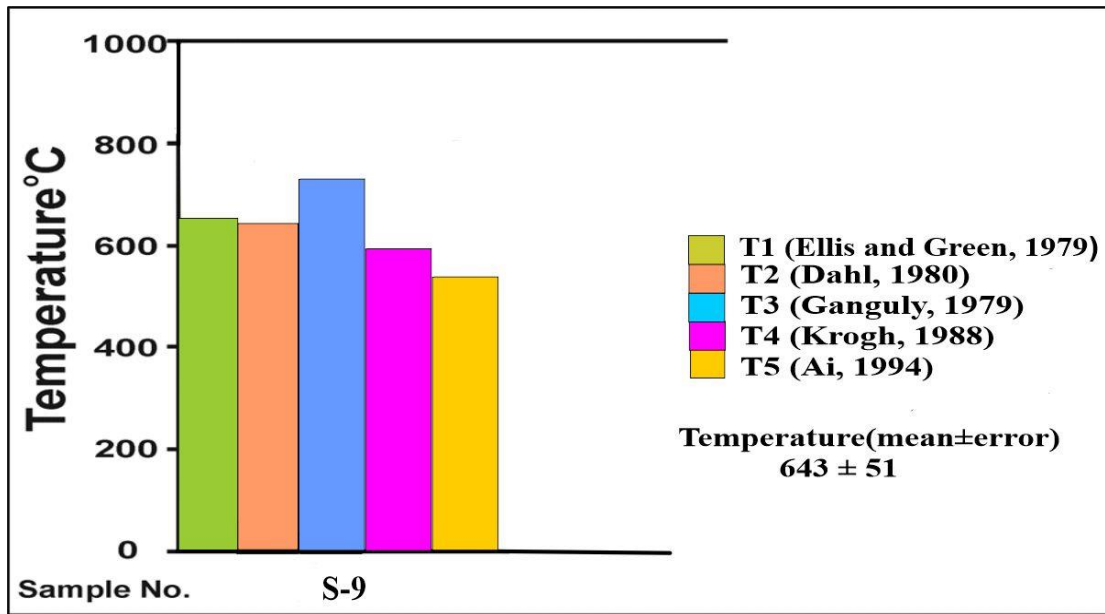


Figure 7.9 Coexisting Garnet-clinopyroxene pairs and derivative temperatures for garnetiferous amphibolites.

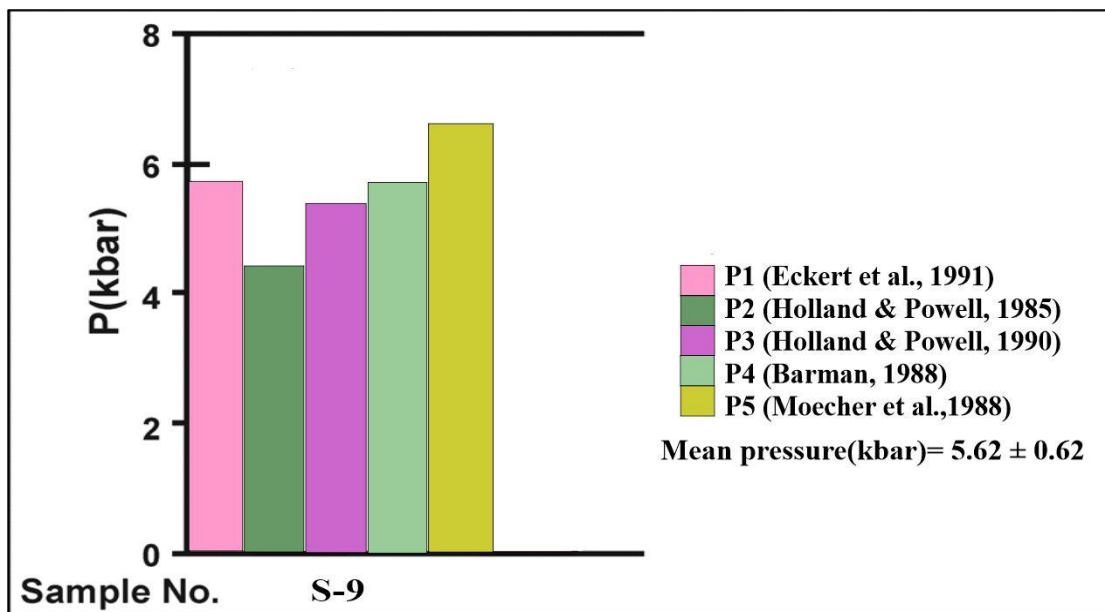


Figure 7.10 Coexisting Garnet-clinopyroxene pairs and derivative pressures for garnetiferous amphibolites.

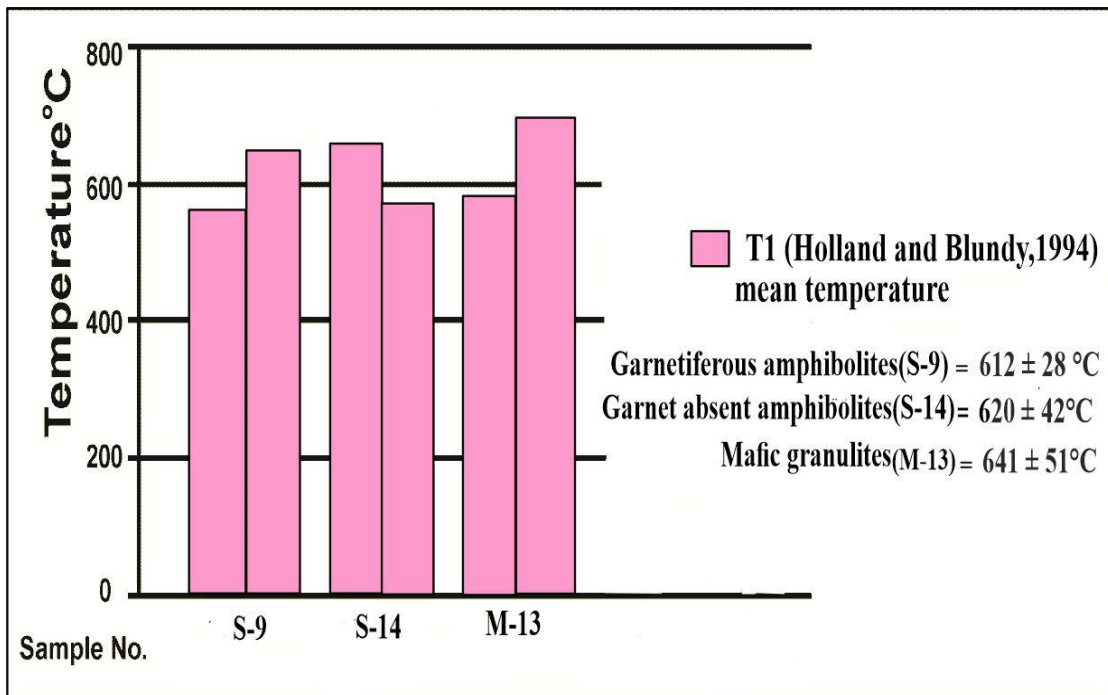


Figure 7.11 Coexisting Amphibole-plagioclase pairs and derivative temperatures for different rocks.

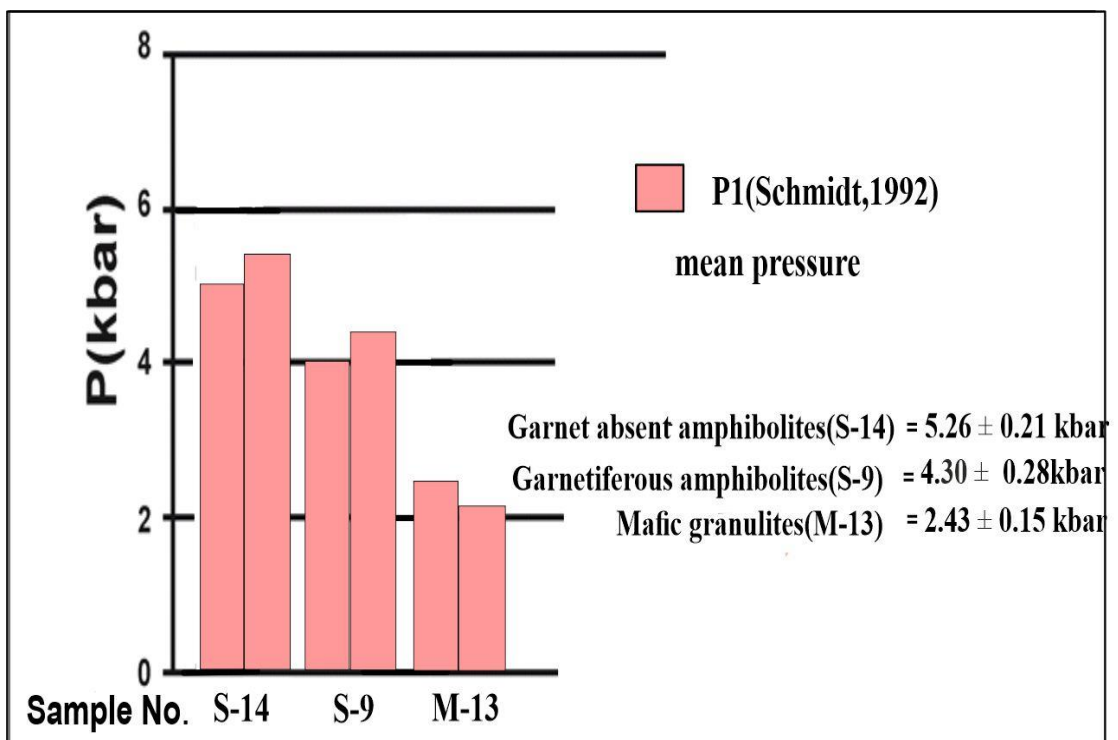


Figure 7.12 Coexisting Amphibole-plagioclase pairs and derivative pressures for different rocks.

Metamorphic Condition

Table 7.1 Results of P–T (pressure–temperature) estimation for pelitic granulites (K-1) and garnet bearing gneisses (M-1) from the study area.

Gt-Bt geothermometer (°C)	6 kbar	6 kbar	Gt-Crd geothermometer (°C)	5kbar
Models	K-1	M-1	Models	K-1
1. Thompson (1976)	727	594	1. Thompson (1976)	568
2. Goldman and Albee (1977)	541	518	2. Holdaway and Lee (1977)	564
3. Holdaway and Lee (1977)	688	574	3. Wells (1979)	536
4. Lavrent'eva and Perchuk (1981)	687	596	4. Dwivedi, Mohan, and Lal (1998)	578
5. Ferry and Spear (1978)	748	571	5. Perchuk et al. (1985)	568
6. Hodges and Spear (1982)	761	588	6. Bhattacharya et al. (1988)	637
7. Ganguly and Saxena (1984)	747	502	Average	575 ± 28
8. Perchuk and Lavrent'eva(1983)	669	579	Gt-Crd-Sil-Qz Barometer(kbar)	600°C
9. Perchuk et al. (1985)	686	602	Models	K-1
10. Dwivedi et al. (2007)	658	486	1. Thompson (1976)	5.73
11. Bhattacharya et al. (1988)	647	562	2. Holdaway and Lee (1977)	6.43
12. Williams & Grambling (1990)	723	621	3. Wells & Richardson (1979)	6.04
Average	690 ±62	566 ±33	4. Perchuk et al. (1985)	3.35
Gt-Bt-Pl-Qz geobarometer (kbar)	600°C	600°C	5. Wells (1979)	6.2
Model	K-1	M-1	6. Dwivedi, Mohan, and Lal (1997)	5.56
1. Hoisch(1990)	6.2	5.11	Average	5.55 ± 0.73
Result of internally consistent dataset				
(Thermocalc v 3.21) a (H ₂ O) = 1				
(P–T) av 679 ± 63 °C/5.3 ± 0.9 Kbar				
Independent set of reactions used to estimate (PTav)				
(For a (H ₂ O) = 1)				
1. py + 2gr + 3east + 6q = 3phl + 6an				
2. py + 2alm + 3east + 9q = 3phl + 3fcrd				
3. alm + east + 3q = ann + crd				
4. 3py + 2ann + 3east + 9q = 5phl + 3fcrd				

Table 7.2 Results of P–T (pressure–temperature) estimation for mafic granulite samples from the study area.

Opx-Cpx geothermometers	T(°C) at 6 kbar
Peak stage	
Wood & Banno (1973)	815
Wells (1977)	861
Powell (1978)	984
Average	887 ± 62
Opx-Cpx geobarometers	P(kbar) at 887°C
Mercier et.al. (kbar)	5.83-6.47 kbar
Amp-Pl-Qz thermobarometer	
Post Peak stage	
P Schmidt (1992)	2.14 - 2.43 kbar
T (HB1) at pressure by Schmidt (1994)	590-693°C
Result of internally consistent dataset (Thermocalc v 3.21)	a (H ₂ O) = 1
(P–T) average	799± 40 °C/6.3 ± 0.9 kbar
Independent set of reactions used to estimate average (P-T average).	
1. 2fact + 5mgts + 5di + 5q = 2tr + 5 fs + 5an	
2. 2fact + 2mgts = en + 4fs + 2hed + 2an + 2H ₂ O	
3. 3mgts + 3hed + ann + 3q = 3fs + phl + 3an	
4. parg + 4mgts + 5hed + 9q = fact + 4en + 5an + ab	
5. 2parg + 6hed + 8 east + 16 q = 3 fs + 8phl + 10 an + 2ab + 2H ₂ O	

Metamorphic Condition

Table 7.3. Results of P–T (pressure–temperature) estimation for calc-silicate granulites samples from the study area.

Grt-Cpx geothermometers		T(°C) at 7 kbar
-		
(Ellis & Green, 1979)		833
(Dahl, 1980)		573
(Ganguly, 1979) by (Ganguly et al., 1987)		721
(Krogh, 1988)		553
(Yang Ai, 1994)		694
Average		675±89
Grt-Cpx-Pl-Qz geobarometers		P(kbar) at 600 °C
-		
(Eckert et al., 1991)		5.95
(Holland & Powell, 1985)		4.47
(Holland & Powell, 1990)		5.59
(Berman, 1988)		4.76
(Moecher et al., 1988)		6.98
Average		5.55±0.74
Result of internally consistent dataset (Thermocalc v 3.21)		a (H ₂ O) = 0.5
(P–T) average	624 ± 97 °C/5.6 ± 0.8kbar	
Independent set of reactions used to estimate average (P-T average).		
1. 2gr + alm + 3q = 3hed + 3an		
2. alm + 8cz + 5q = 3hed + 13an + 4H ₂ O		
3. alm + 2andr + 4cz + 3q = 3hed + 3an + 4ep		

Table 7.4 Results of P–T (pressure–temperature) estimation for garnetiferous amphibolite (S-9) and garnet absent amphibolite (S-14) samples from the study area.

Grt-Cpx geothermometer (°C)	5 kbar	Grt-Cpx-Pl-Qz Barometer (in Kbar)	600°C
Models	S-9	Models	S-9
1. (Ellis & Green, 1979)	661	1. (Eckert et al., 1991)	5.79
2. (Dahl, 1980)	655	2. (Holland & Powell, 1985)	4.31
3. (Ganguly, 1979) by (Ganguly et al., 1987)	740	3. (Holland & Powell, 1990)	5.43
4. (Krogh, 1988)	599	4. (Berman, 1988)	5.86
5. (Yang Ai, 1994)	558	5. (Moecher et al., 1988)	6.72
Average	643±51	Average	5.62±0.62
Hbl-Pl-Q thermobarometer	S-9	Hbl-Pl-Q thermobarometer	S-14
Post Peak stage		Post Peak stage	
P Schmidt (1992)	4.02-4.58 kbar	P Schmidt (1992)	5.05-5.47kbar
T (HB1) (1994)	585 - 640°C	T (HB1) (1994)	578 - 663°C
Result of internally consistent dataset(S-9)		Result of internally consistent dataset (S-14)	
(Thermocalc v 3.21) a (H ₂ O) = 1		(Thermocalc v 3.21) a (H ₂ O) = 1	
(P–T) av 706 ± 63 °C/5.5 ± 0.9 kbars		(P–T) av 616 ± 81 °C/5.2 ± 0.7 kbars	
Independent set of reactions used to estimate (PTav)		Independent set of reactions used to estimate (PTav)	
(For a (H ₂ O) = 1):		(For a (H ₂ O) = 1):	
1. py + 2gr + 3q = 3an + 3di		1. ts + 2di + 2q = 2an + tr	
2. 2gr + alm + 3q = 3an + 3hed		2. 5ts + 10hed + 10q = 10an + 3tr + 2fact	
3. 2py + 4gr + 3ts + 12q = 12an + 3tr		3. east + ts + 3hed + 3q = ann + 3an + tr	
4. 21an + 6tr = 10py + 11gr + 27q + 6H ₂ O		4. 4ann + 3parg + 3hed + 15q = 4phl + 3an + 3ab + 3fact	
5. 4gr + 5alm + 3ts + 12q = 3py + 12an + 3fact		5. 10ab + 25ts + 40hed = 40an + 7tr + 8fact + 10parg	
6. 2py + 4gr + 3gl + 12q = 6an + 6ab + 3tr			
7. 7py + 21east + 12fact = 8gr + 20alm + 21phl + 12q + 12H ₂ O			
8. 5alm + 12an + 3parg + 18di = 10py + 10gr + 3ab + 3fact			
9. 3alm + 3east + 6di = 4py + 2gr + 3ann			

PART C- BULK COMPOSITION MODELLING

7. C.1 Application of equilibrium thermodynamic

Progress in comprehending the thermodynamic behaviour of metamorphic phases, encompassing both primary and accessory constituents in rocks (Powell and Holland, 1985; Berman, 1988; Holland and Powell, 1998) has enabled the computation of average crystallization conditions and quantitative phase diagrams for mineral systems believed to capture chemical equilibrium. This method proves valuable for determining the pressure-temperature pathways of metamorphic rocks that have been exhumed. The achievement of geologically accurate relations involving pressure, temperature, and composition from metamorphic rocks hinges on the demonstration that the phases within the system (i.e., mineral assemblage) indeed represent a state of thermodynamic equilibrium. Given that metamorphism is a dynamic process characterized by changing P, T, and X throughout a metamorphic evolution of rock, the assumption of chemical equilibrium remains uncertain. The kinetics of intergranular diffusion play a crucial role in determining the time and length scales of metamorphic equilibration (Carlson, 2011). Detailed knowledge regarding intergranular diffusion rates for both major and trace elements is still lacking. However, the presence of an intergranular fluid phase accelerates the rates of elemental exchange and consequently, metamorphic equilibration (Carlson, 2002). As a result, prograde dehydration metamorphic reactions proceed more rapidly than retrograde hydration reactions, explaining the common preservation of mineral assemblages formed under peak temperature conditions. This observation aligns with predictions from phase equilibrium modelling and observed metamorphic mineral

assemblages. Despite theoretical support for the equilibrium condition, commonly observed features like coronal texture (Johnson and Carlson, 1990), pseudomorphous growth structures (Foster, 1986) and linked segregations (Carmichael, 1969) provide petrographic evidence of chemical disequilibrium, where reactions halt before complete consumption of reactants. Such evidence is frequently found in H₂O under under-saturated conditions, indicating sluggish intergranular diffusion kinetics. Consequently, it is significant to examine samples for petrographic signs of disequilibrium before applying equilibrium thermodynamic principles. The validity of the equilibrium model of metamorphism cannot be proven. Instead, the absence of disequilibrium features is typically considered supporting evidence. Moreover, equilibrium mineral assemblages must adhere to the phase rule ($F = C + 2 - P$, where P = number of phases present, C = number of components, and F = variance) and demonstrate consistent element partitioning between co-genetic phases.

Upon accepting the valid application of equilibrium thermodynamics to metamorphic rocks, thermodynamic descriptions of relevant phases are coupled with activity-composition models ($a-x$) describing the energetics of end-member phase interaction (Helgeson et al., 1978). This allows for the calculation of peak Pressure-Temperature conditions for the given mineral assemblage. Initially, this approach was limited to precisely calibrated reactions (Ferry and Spear, 1978), and later expanded to consider numerous reactions enabling the estimation of average P-T conditions (Powell and Holland, 1988). However, this geothermobarometry is constrained by its dependence on mineral chemistry, inherent to the inverse nature of the method. Advancements in the quality and scope of the thermodynamic dataset and $a-x$ relations based on the same phase end-member compositions (internally consistent

Metamorphic Condition

datasets – Powell & Holland, 1988, Holland and Powell, 1990, 1998) formed the basis for developing forward phase equilibria modelling. In this approach, given a reactive composition, relations involving P-T, P- X, or T-X (pseudosections) can be determined for all phases in the system of interest.

7.C.2 Pseudosection modelling

Pseudosection modelling stands as the most potent technique for extracting pressure-temperature data from metamorphic rocks that have undergone exhumation (Powell et al., 1998; Powell and Holland, 2010). The concept of pseudosections emerged from the development of petrogenetic grids, which delineate all invariant points and univariant lines across all mineral phases and bulk compositions within a chemical system (Powell and Holland, 1990). These petrogenetic grids furnish information about the absolute stability of mineral assemblages but do not provide details regarding phase composition and abundance. Pseudosections modelling, on the other hand, offer a means to adapt the petrogenetic grid for a specific bulk composition, effectively creating a mineral assemblage map in P-T-X space (Powell et al., 1998). The reliability of the pseudosection modelling approach hinges on accurately determining the reactive bulk composition. As previously discussed, the length scales associated with diffusive equilibration remain poorly constrained in metamorphic rocks presenting a significant inherent uncertainty in this technique. Pseudosection Modeling of rocks containing zoned porphyroblasts poses particular challenges, as the effective bulk composition evolves with porphyroblast growth, causing variations in pseudosection topology over time. This phenomenon is exemplified by garnet growth, which preferentially incorporates Manganese during its

early growth stages (Mahar et al., 1997). To address reactive volume fractionation, it is possible to select a garnet composition, typically ranging from the core (initiation of growth) to the rim (cessation of growth) to calculate the bulk composition of the rock. The pseudosection modellings presented in this chapter rely on bulk compositions calculated by combining mineral proportions unless specified otherwise.

7.C.3 Methodology

The phase diagram was computed using the *Perple_X* 6.8.2 software package, which has various sub-programs. A pseudosection modelling is a diagram illustrating various reaction conditions within the P-T space, adapted to a specific bulk composition. The bulk rock compositions for pseudosection calculations were determined from whole-rock X-ray fluorescence (XRF) analyses conducted at the Birbal Sahni Institute of Palaeosciences (BSIP) in Lucknow, India. The process typically involves running the build program with computational option files, after that the Vertex program computes the phase diagram. Detailed information about solution models can be found in the "*Perple_X* Updates" and "*Perple_X* solution model glossary" (http://www.perplex.ethz.ch/perplex_updates.html). Subsequently, the Pssect program is executed which may require a considerable amount of time to generate a postscript plot. The final diagrams are then refined using other graphic editing software and isopleths are generated using the Pywerami program.

7.C.4 Pelitic granulite

The P-T pseudosection in the NCKFMASH model system was estimated based on bulk composition to constrain the peak and retrograde history of the Pelitic granulites. The *Perple X* software (version. 6.8.2; Connolly, 2005,2009) was used

Metamorphic Condition

with the solid solution models such as cordierite, garnet, melt (W: White, 2014); biotite (TCC: Tajcmanová, 2009) plagioclase (HP: Holland and Powell, 2003), as well as pure end-member phases of H₂O and quartz. The average chemical composition of the Pelitic granulite sample in mol % is SiO₂ = 68.87, Al₂O₃ = 7.55, CaO = 3.30, FeO = 8.47, K₂O = 1.29, MgO = 4.97, Na₂O = 2.30 and H₂O = 2.6. MnO, TiO₂ and P₂O₅ contents are very low, hence it is neglected in pseudosection construction, whereas P₂O₅ is used in a recalculation of CaO. Pelitic granulites contain a leucosome band indicating the availability of melt so it is considered in the bulk composition modelling. T-X pseudosection is constructed at 6 kbar pressure to constrain the molar composition of H₂O (Fig. 7.13). The molar composition of H₂O ranges from anhydrous (X = 0.0 mol %) to excess H₂O composition (X = 6.0 mol %) and is plotted along the X axis. The molar composition of H₂O (X=2.6 mol%) is a suitable constituent for the formation of stable mineral assemblages such as (Gt-Bt-Crd-Sil-Pl-Qz). The P-T pseudosection is constructed in the range of 650-900 °C and 4.5-7.5 kbar. Garnet and sillimanite-bearing mineral assemblage exhibit peak metamorphic assemblages that dominate at higher pressure, however, cordierite-bearing mineral assemblages are stable at lower pressures in the P-T pseudosection modelling. The equilibrium mineral assemblage (Gt-Bt-Crd- sil-Pl-Qz-melt) estimated for the pelitic granulite lies in the P-T range of 730 -765°C to 5.1- 6.3 kbar (Fig. 7.14). The X_{Mg} isopleths of garnet, biotite and cordierite are computed to analyse their nature with variations in Pressure-temperature and other mineral assemblages in the equilibria field. It has been observed that the trivariate mineral equilibria (Gt-Sil-Bt -Pl-Qz-Melt) show peak mineral equilibria that are Cordierite absent assemblages. The X_{Mg} isopleths of garnet rises with increasing Temperature. However, in the divariant

mineral equilibria field (Gt-Crd-Bt-Sil- Pl-Qz- melt) with two trivariant mineral equilibria field (Gt-Bt-Sil-Pl-Qz-melt) and (Gt-Crd-Pl- Sil-Qz-melt), the X_{Mg} isopleths of garnet rises with increasing pressure. The peak mineral assemblage (Gt-Bt- Sil-Pl-Qz-melt) was stable in the P-T range of 740–750 °C and 6.7–7.4 kbar. By contouring the X_{Mg} isopleth line of garnet and biotite, this peak metamorphic condition has been determined (Fig. 7.14). The retrograde mineral assemblage (Gt-Crd- Bt -Pl-Qz-melt) formed during post-peak (M2) metamorphism, lies in the P–T range from 725 -730 °C and 4.5 - 4.7 kbar are derived by contouring X_{Mg} isopleths of garnet and cordierite.

Table 7.5 Whole-rock data of pelitic granulite (K-1) from the study area.

Wt%	SiO₂	Al₂O₃	TiO₂	FeO	MnO	MgO	CaO	Na₂O	K₂O	P₂O₅	LOI
	65.24	12.14	0.81	10.24	0.07	3.16	2.92	2.25	1.91	0.21	0.86
Mol%	SiO₂	Al₂O₃	TiO₂	FeO	MgO	CaO	Na₂O	K₂O	H₂O		
	68.46	7.51	0.64	8.99	4.94	3.28	2.29	1.27	2.60		

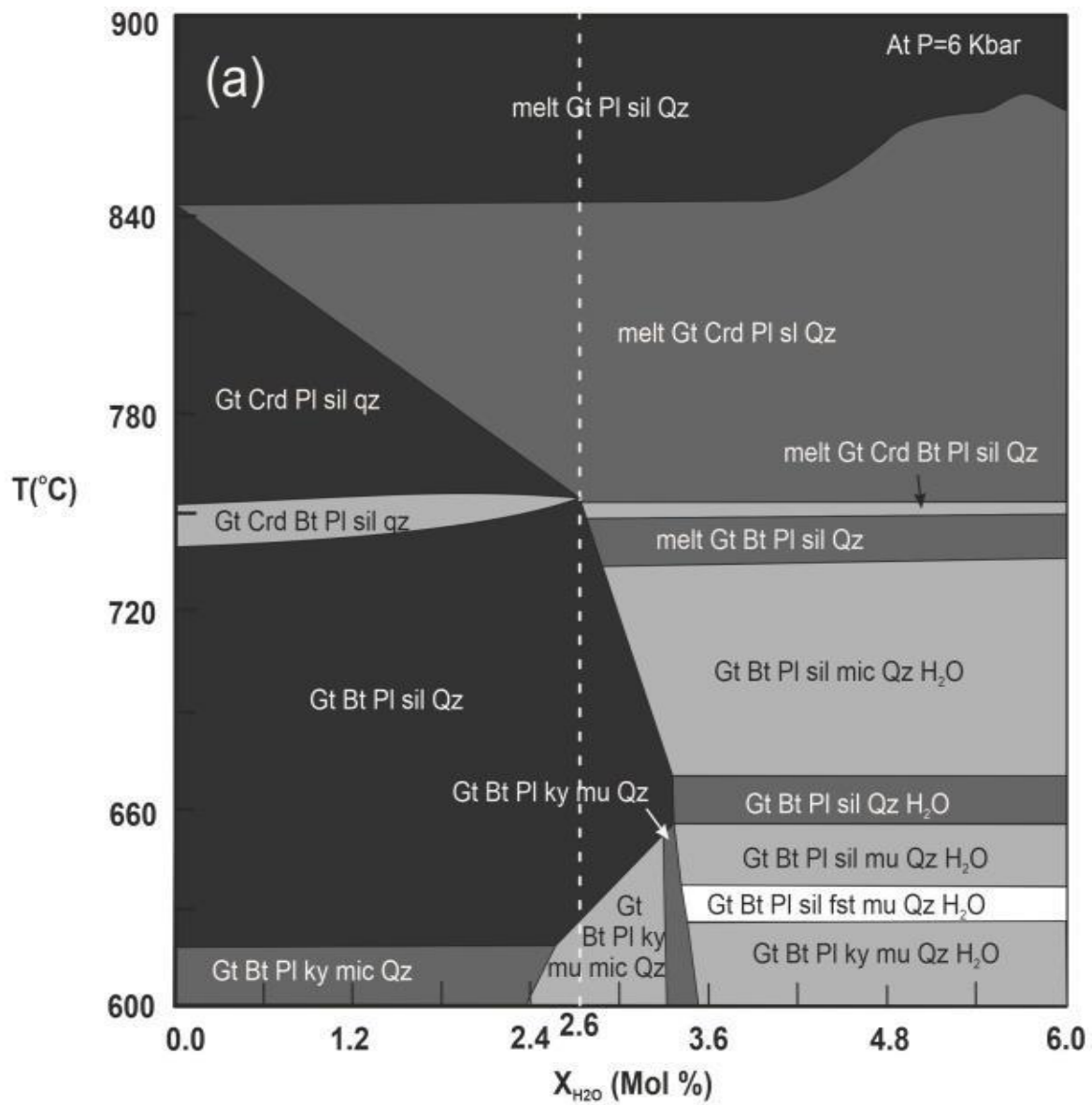


Figure 7.13 T-X(H₂O) Pseudosection calculated at fixed pressure 6 kbar, showing the effects of varying the molar proportions of bulk-rock H₂O in pelitic granulites (sample K-1). The white dashed line shows the modelled composition of H₂O (2.60 mol%).

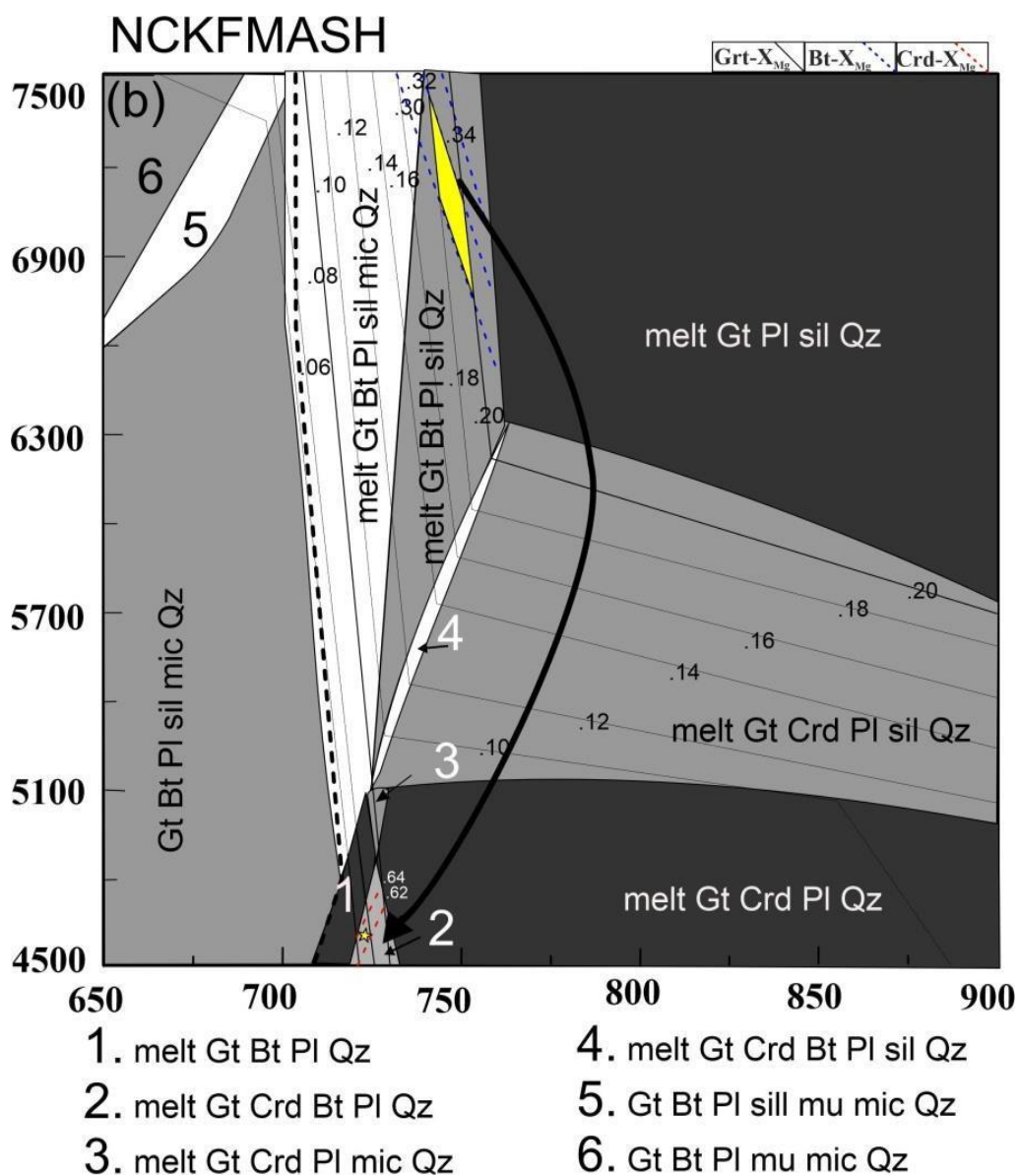


Figure 7.14 P–T pseudosections for pelitic granulite (sample K-1), showing the peak and post-peak metamorphic condition and isopleth of garnet, biotite and cordierite are contoured in the P–T pseudosection.

7.C.5 Mafic granulite

The representative mafic granulite sample (M-13) was analyzed using *Perple_X* version 6.8.2 software (Connolly 2005, 2009) along with thermodynamic data from Holland and Powell (1998, 2011) to generate pseudosections. These P–T pseudosections for the mafic granulite were computed within the (Na₂O–CaO–K₂O–FeO–MgO–Al₂O₃–SiO₂–H₂O–TiO₂–O) system (NCKFMASHTO) system, which is

Metamorphic Condition

well-suited for bulk composition modelling of the rock being studied. There are different solution models used for construction the of pseudosection; clinopyroxene, orthopyroxene (Holland and Powell, 2003), biotite (Tajcmanova et al., 2009), amphibole (Diener et al., 2007), plagioclase (Fuhrman & Lindsley, 1988), ilmenite (White et al., 2000), melt (White et al., 2014) including some of the pure end-member phases associated withit such as quartz. The measured bulk rock composition of mafic granulite (M-13), normalized in mol%, is as follows: SiO₂ = 52.22, Al₂O₃ = 6.90, CaO = 10.14, FeO = 14.68, K₂O = 0.49, MgO = 8.94, Na₂O = 2.22, TiO₂ = 0.69, H₂O = 2.9 and O = 0.81 (Table 7.6). MnO was ignored in the model system as it constituted only a small proportion of the total rock. The O₂ (Fe₂O₃) was evaluated by integrating mineral compositions and modal abundance data of the phases presented in the rock. H₂O content was recovered based on the amounts of hydrous mineral phases in biotite and amphibole. Biotite (~3–4 wt% H₂O) and amphibole (~2.5–3.5 wt% H₂O) constituted about 5% and 20% of the total rock volume, respectively; therefore, it was suggested that ~ 0.9 wt% H₂O for bulk rock composition. The P–T pseudosection for the sample was calculated over a temperature range of 3–8 kbar and 750–900 °C (Fig.7.15). Quartz is stable at high pressure, K-feldspar is stable below 820°C and magnetite is stable at lower pressures. Biotite is stable at temperatures lower than about 840 °C and pressures less than about 7.0 kbar (Fig.7.15). The equilibrium mineral assemblage's orthopyroxene – clinopyroxene – hornblende–biotite-plagioclase–ilmenite, which we got from petrographic analysis, lie in the P-T range of 5.2 to 6.4 kbar and 810 to 850 °C. The peak metamorphic assemblage of orthopyroxene – clinopyroxene – hornblende–plagioclase – ilmenite –melt was stable in the P-T range of 835 and 870°C at 5.0 – 6.9 kbar (Fig. 7.15).

7.C.6 Calc-silicate granulite

The Isobaric T–X (CO₂) pseudo section in the NCFMAST-HC model system was estimated based on bulk composition to constrain the mole fraction of CO₂ and temperature condition of equilibrium mineral assemblage (GrtCpx-Sph-Cz-Pl). Calc-silicate granulite sample (M-7) was derived with the help of Perple_X ver.6.8.2 software (Connolly 2005, 2009) and the end-member thermodynamic dataset Holland and Powell (1998, 2011). The phases that are used in the modelling are Clinopyroxene (HP: Holland & Powell, 1998); Garnet (HP: Holland & Powell, 1998); melt (W: White et al., 2014); feldspar (feldspar: Fuhrman and Lindsley, 1988), as well as some pure endmember phases of sphene, clinozoisite, chlorite, quartz CO₂ and H₂O. The average chemical composition of the calc-silicate granulite sample in mol% is: SiO₂ = 49.60, Al₂O₃ = 6.92, CaO = 23.52, FeO = 9.94, MgO = 7.74, Na₂O = 1.04, TiO₂ = 1.15 (Table 7.7). MnO, K₂O and P₂O₅ contents are very low, hence it is neglected in pseudosection construction, whereas P₂O₅ is used in a recalculation of CaO. The mole fraction of CO₂ ranges from (XCO₂ = 0) to (XCO₂ = 1) and is plotted along the X-axis. The Isobaric T–X (CO₂) pseudosection is constructed in the range of 300-800 °C and at a fixed pressure of 7 kbar. The mole fraction of CO₂ (XCO₂ > 0.4) is a suitable constituent for the formation of stable mineral assemblage such as (Grt-Cpx-Sph-Cz-Pl) along with a temperature range from 620 -635°C (Fig. 7.16).

Table 7.7 Whole-rock data of calc-silicate granulite (M-7) from the study area.

Wt%	SiO₂	Al₂O₃	TiO₂	FeO	MnO	MgO	CaO	Na₂O	K₂O	P₂O₅	LOI
	47.28	11.19	1.46	11.33	0.05	4.95	20.93	1.02	0.04	0.07	1.58
Mol%	SiO₂	Al₂O₃	TiO₂	FeO	MgO	CaO	Na₂O	K₂O			
	49.60	6.92	1.15	9.94	7.74	23.52	1.04	0.03			

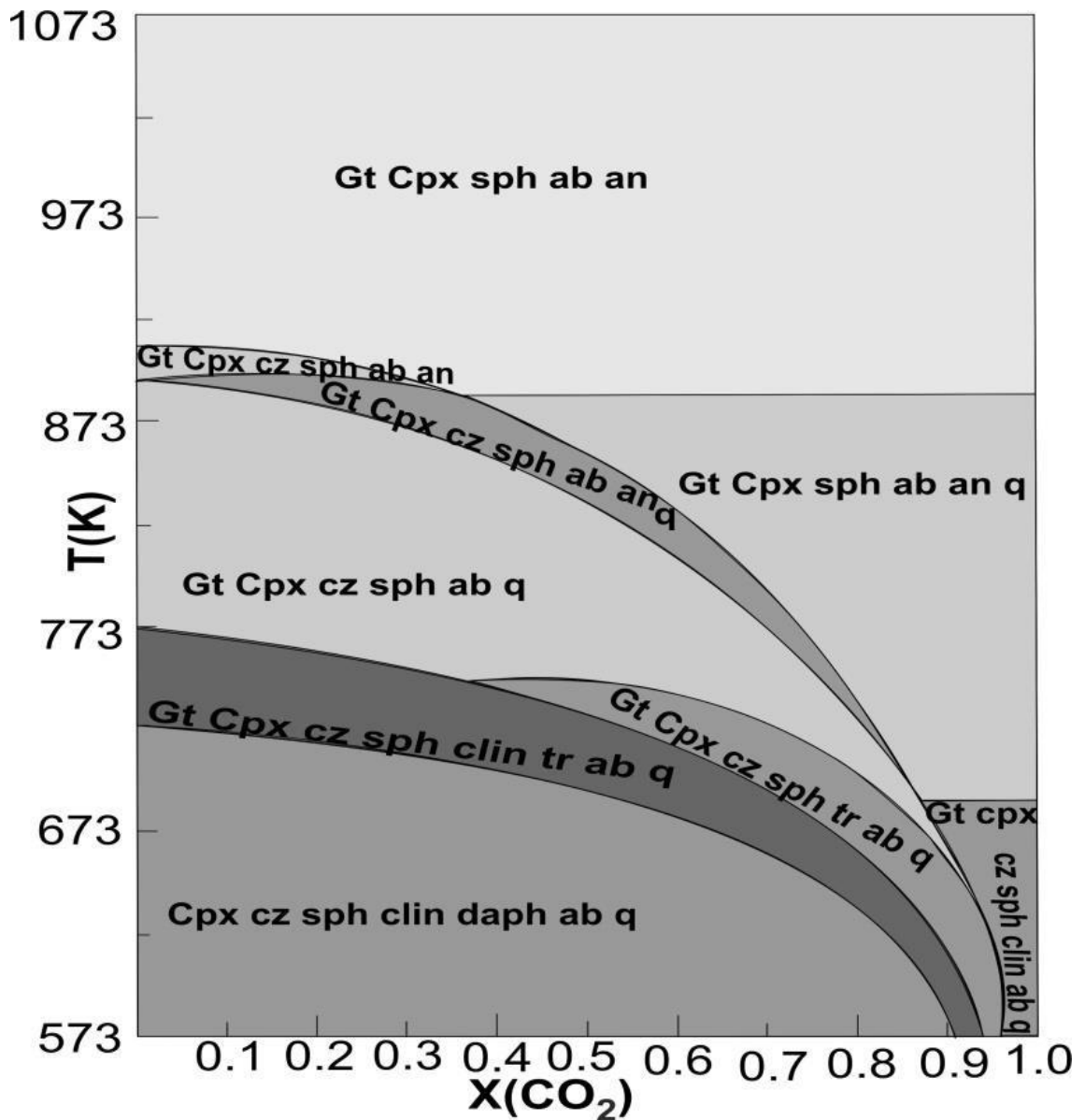


Figure 7.16 The T- X_{CO_2} pseudosection for calc-silicate granulite (M-7) from the study area was calculated in the NCFMAST-HC model system using the Perple_X software.

7.C.7 Garnetiferous amphibolite

Pseudosection of the representative garnetiferous amphibolite sample (S-9) was derived with the help of Perple_X ver.6.8.2 software (Connolly 2005, 2009) and end-member thermodynamic dataset Holland and Powell (1998, 2011). The assumed values for H_2O have been determined by the constructed T-X (H_2O) pseudosection at a constant pressure of 5.0 kbar for the garnetiferous amphibolite sample (S-9)

Metamorphic Condition

(Fig.7.17). The H₂O value was derived based on the range of H₂O content in the bulk rock composition, spanning from 0.0 to 6.0 mol% and in the T-X (H₂O) diagram peak and post-peak mineral assemblages are represented, with the appropriate amount of X (H₂O) = 4.30 mol%. The pseudosection modeling employed activity composition models for various minerals, including clinopyroxene, (Holland & Powell, 2003), amphibole (Diener et al., 2007), biotite (Tajcmanova et al., 2009), plagioclase (Fuhrman & Lindsley, 1988), and ilmenite (White et al., 2000). Given the low levels of MnO and P₂O₅, they were not taken in the construction of the pseudo section. The measured whole-rock composition of garnetiferous amphibolites (S-9), normalized in mol%, is as follows: SiO₂ = 52.23, Al₂O₃ = 8.61, CaO = 10.34, FeO = 11.40, K₂O = 1.31, MgO = 7.04, Na₂O = 2.37, TiO₂ = 1.34, H₂O = 4.30 and O = 0.96 (Table 7.8).

The P–T pseudosection for garnetiferous amphibolites (S-9) was generated within the pressure-temperature range of 3–9 kbar and 400–900°C, using the NCKFMASHTO system (Fig.7.18). The mineral assemblages identified through petrographic observations consist of garnet, amphibole, clinopyroxene, plagioclase, biotite, quartz, and ilmenite. The stability of clinopyroxene is pressure-dependent and stable at higher temperatures while garnet becomes more stable at higher pressures. Isopleth lines representing garnet, amphibole, clinopyroxene, and biotite help define the specific P–T conditions associated with these stages (Fig. 7.18). The assemblage marks the peak metamorphic stage for garnetiferous amphibolite is Grt-Amp-Cpx- Bt-Pl-Qz-Ilm-H₂O. It occurs under higher P–T conditions, specifically 7.1–7.3 kbar/790–810 °C. After peak metamorphism, garnet and clinopyroxene are consumed, giving way to amphibole formation during retrograde metamorphism. The post-peak metamorphic assemblage exhibits fewer mineral constituents, including Amp-Bt-Pl-

Qz- Ilm, and is stable within a P-T range of 6.10–4.10 kbar and 760–590°C. Amphibole and biotite isopleths delineate the conditions for post-peak metamorphism more specifically at 4.10–4.50 kbar/590–610°C.

Table 7.8 Whole-rock data of garnetiferous amphibolite (S-9) from the study area.

Wt%	SiO ₂	Al ₂ O ₃	TiO ₂	Fe ₂ O ₃	MnO	MgO	CaO	Na ₂ O	K ₂ O	P ₂ O ₅	LOI
	50.45	14.12	1.72	13.17	0.22	4.56	9.32	2.36	1.98	0.12	1.28
Mol%	SiO ₂	Al ₂ O ₃	TiO ₂	FeO	MgO	CaO	Na ₂ O	K ₂ O	O ₂	H ₂ O	
	52.23	8.61	1.34	11.4	7.04	10.34	2.37	1.31	0.96	4.3	

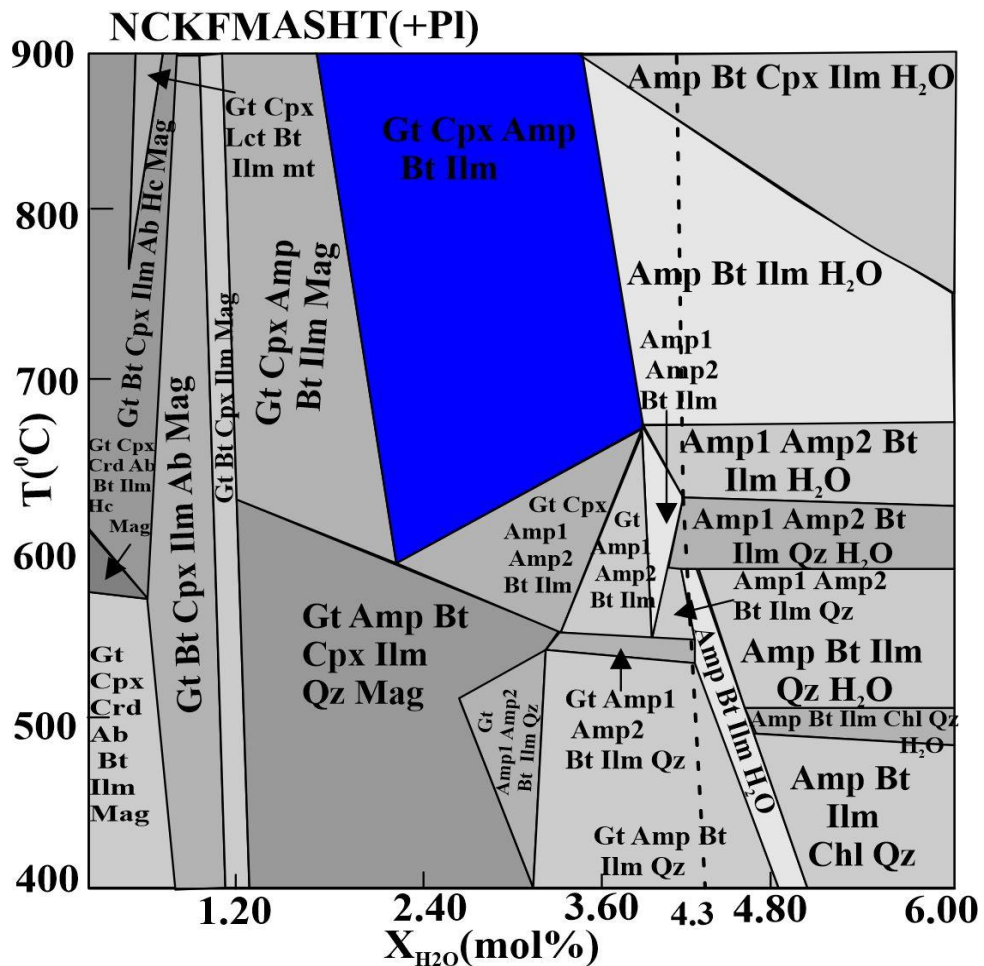


Figure 7.17 The T-X (H₂O) Pseudosection was computed at a constant pressure of 5.0 kbar, illustrating how changes in the molar proportions of H₂O in garnetiferous amphibolites (sample S-9) impact the system. The black dashed line represents the modelled composition of H₂O at 4.3 mol% and blue shading is showing the peak mineral assemblage (Gt-Cpx-Amp-Bt-Pl-Ilm).

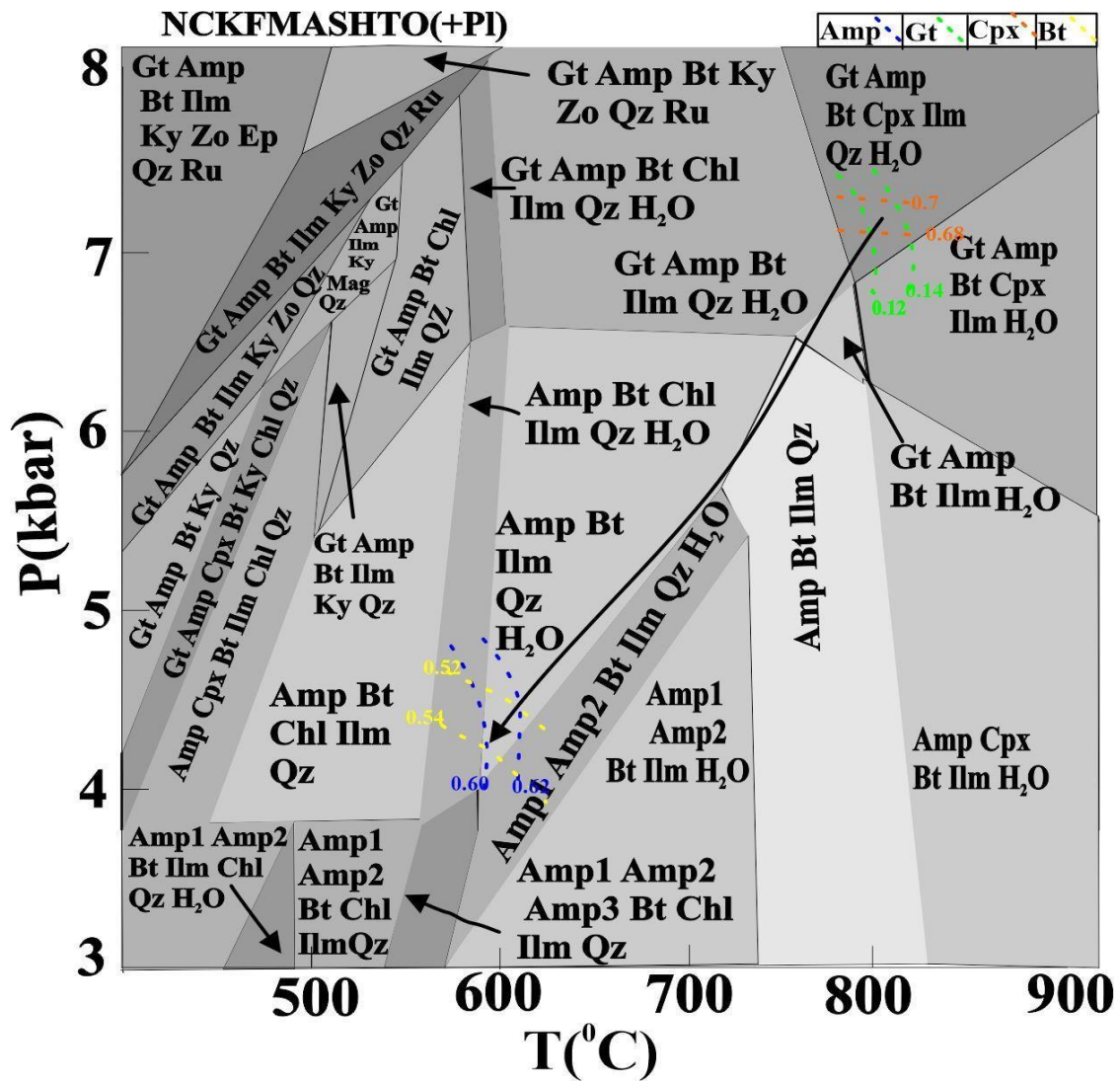


Figure 7.18 A P-T Pseudosection was constructed for garnetiferous amphibolites (sample S-9), revealing various metamorphic conditions including peak and post-peak stages.